

PECULIARITIES OF POLYTHERMIC DECOMPOSITION OF IRON, COBALT AND NICKEL OXALATES WITHIN PORES OF PHOTONIC CRYSTALS BASED ON SiO₂ IN ATMOSPHERE WITH OXYGEN LACK

A. N. Zakharov*, A. F. Mayorova and N. S. Perov

Moscow State Lomonosov University, Moscow, Russia

Iron(II), cobalt(II) and nickel(II) oxalates were synthesized as nanofractals inside the voids of the photonic crystals based on SiO₂. Guest substances undergone polythermic decomposition within the pores of the photonic crystals in helium atmosphere containing of oxygen traces (~1 Pa) under static conditions. Pyrolysis of Fe(COO)₂·2H₂O, Co(COO)₂·2H₂O and Ni(COO)₂·2H₂O studied by TG and DSC techniques results in the formation of the metal oxides. The nanoparticles of Fe₂O₃, CoO (Co₃O₄) and NiO populated the interspheric voids of the photonic crystals exhibited no ferromagnetic effects indicating that no metallic inclusions were formed in helium in the presence of O₂ traces. The exothermic effect was observed by the thermal decomposition of the cobalt(II) oxalate only under oxygen lack.

Keywords: cobalt oxalate, decomposition, interspheric voids, iron oxalate, nickel oxalate, photonic crystals

Introduction

Topochemical reactions within pores of crystal materials are used for modification of solids by inclusions of metals or its oxides. Photonic crystals (PC) based on SiO₂, synthetic opals, populated with ferromagnetic fractals were applied to a construction of weak magnetic field sensors, in systems for record and store of information, and other nanotechnological branches.

Experimental

Materials

Iron(II), cobalt(II) and nickel(II) oxalates were prepared in situ by reactions of (NH₄)₂Fe(SO₄)₂·6H₂O (Sigma-Aldrich Chemical Co.), Co(NO₃)₂·6H₂O (Aldrich), NiCl₂·6H₂O (Aldrich) with H₂C₂O₄ (Aldrich) according to [1]. Acetone and ethanol have been purified by fractional distillation under atmospheric pressure.

Photonic crystals based on amorphous polycondensed SiO₂ were synthesized by Guryanov. PC were precalcined at 800 K for 5 h. Metal(II) oxalates were synthesized within interspheric voids of dehydrated PC according to [1].

Methods

The supported samples were heated in helium containing remaining oxygen (~1 Pa) in a static system

under a linearly-programmed temperature. The rates of heating were 2, 5 and 10 K min⁻¹. The mass loss and thermal effects were monitored by TG and DSC techniques (Netzsch thermal analyzer STA 409).

Magnetic moment measurements were carried out at room temperature using a vibrating sample magnetometer (accuracy of 8·10⁻¹¹ A m²) in the range from -800 to 800 kA m⁻¹.

Results and discussion

Thermal transformations of iron(II), cobalt(II) and nickel(II) oxalate dihydrates were studied elsewhere under variable conditions [2–7]. The topochemical M(COO)₂·2H₂O (M=Fe, Co, Ni) decomposition was observed to undergo two-step reactions. On the first step, the dehydration (1) takes place.



The decomposition of the anhydrous materials was found to be dependent on many factors such as the nature of the metal and gas phase, shape and dimensions of the sample particles, prehistory of the sample preparation, the conditions of the decay and so on [3]. The pyrolysis of the dehydrated metal(II) oxalates in oxygen or nitrogen containing traces of oxygen was considered to result in the formation of a metal phase according to the reaction (2) or metal oxide (3) depending on the nature of the metal [3].



* Author for correspondence: alxnz@zakhar.msk.ru



Iron(II) and nickel(II) oxalates were found to decompose by a formation of corresponding oxide, Fe_2O_3 (FeO , Fe_3O_4) and NiO .

A concept that the decomposition of $\text{Co}(\text{COO})_2 \cdot 2\text{H}_2\text{O}$ causes to a formation of both CoO and Co in parallel pathways according to the reactions (2) and (3) independent of the nature of the gas phase supported by others [4]. Also, it is unambiguously that the prior dehydration conditions effect upon the subsequent decomposition of the anhydrous material. It was for instance shown [2] that the conditions of $\text{Co}(\text{COO})_2 \cdot 2\text{H}_2\text{O}$ dehydration resulted in variations of particle size and porosity of the anhydrous oxalate and that this has a significant effect on the kinetics of decomposition. The particles of the cobalt oxalate dehydrated in a vacuum at 200°C were of $1\ \mu\text{m}$ in diameter and less and broke up into spherical ones [2]. The dehydration of $\text{Co}(\text{COO})_2 \cdot 2\text{H}_2\text{O}$ at lower temperature revealed more porous and larger particles of about $5\ \mu\text{m}$ diameter.

The porosity of a material to be decomposed is evident to be of great importance for topochemical reactions. Our work reports that the way of the synthesis of $\text{Co}(\text{COO})_2 \cdot 2\text{H}_2\text{O}$ effects the peculiarities of the kinetics of the decomposition and mechanism of the decay.

The thermal behavior of metal oxalates within pores of the photonic crystals based on amorphous polycondensed SiO_2 is unknown. On the one hand, it should be no difference in thermal behavior of the metal(II) oxalates supported on a solid. On the other hand, it is of special importance for solid-phase transformations the dimensions of species to decompose. There are nanospecies of the metal oxalates supported on PC that undergo a topochemical reaction. An average dimension of the metal oxalate particles prepared inside the pores of fcc crystal structure of PC based on SiO_2 is limited by the effective diameter the pores $d \leq D(2/\sqrt{3}-1)$, D is effective diameter of the SiO_2 nanospheres ($\sim 240\ \text{nm}$). We supposed that the parceled phases of the metal oxalates could not exceed $40\ \text{nm}$ in diameter in accordance with a size of the voids of the photonic crystallites.

Table 1 summarizes the characteristics of the samples obtained by a matrix synthesis of the iron(II), cobalt(II) and nickel(II) oxalates. Figure 1 shows representative TG-, DTG- and DSC-traces for temperature-programmed decomposition of supported $\text{Co}(\text{COO})_2 \cdot 2\text{H}_2\text{O}$ up to 500°C in helium under static conditions. There are some stages of a mass loss. The lowest-temperature loss of the mass was due to a dehydration of the photonic crystals. The samples released the main part of adsorbed water in the range of $300\text{--}400\ \text{K}$. The second and third mass losses were connected with the dehydration and decomposition of the cobalt(II) oxalate, respectively. The iron(II) and nickel(II) oxalates supported on the

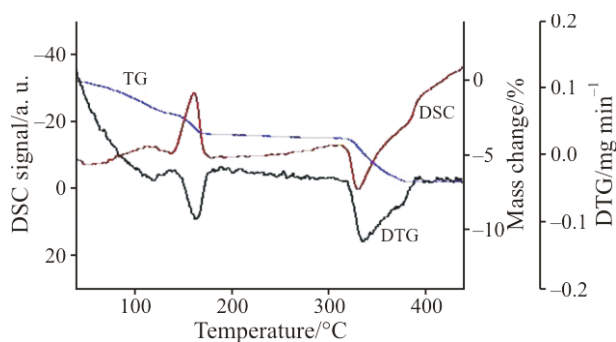


Fig. 1 TG, DTG and DSC plots for the pyrolysis of $\text{Co}(\text{COO})_2 \cdot 2\text{H}_2\text{O}$ supported on the photonic crystals based on SiO_2 (in He); heating rate is $5\ \text{K}\ \text{min}^{-1}$

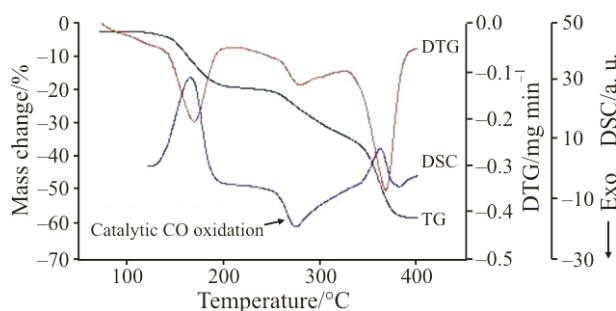
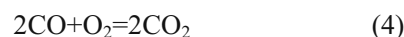


Fig. 2 TG, DTG and DSC plots for the pyrolysis of unsupported $\text{Co}(\text{COO})_2 \cdot 2\text{H}_2\text{O}$ (in He); heating rate is $5\ \text{K}\ \text{min}^{-1}$

Table 1 Characteristics of the samples of the photonic crystals (PC) based on SiO_2 containing $M(\text{COO})_2 \cdot 2\text{H}_2\text{O}$: metal oxalate/photonic crystals mass ratio (r), theoretic (γ_t) and experimental (γ_e) ratio $\gamma = \Delta m_3 / \Delta m_2$ of the mass losses of the 3rd (Δm_3) to the 2nd (Δm_2) steps of the decomposition, by linear-programmed heating in helium

Sample	M^{2+}	$r/\%$	$\beta/\text{K}\ \text{min}^{-1}$	γ_e (γ_t)
1	Fe	0.39	10	2.58 (2.89)
2	Co	6.88	10	2.41 (2.40)
3	Ni	1.07	2	2.38 (2.45)

photonic crystals undergone only endothermic reactions in helium to form the corresponding metal oxides. The decomposition of the supported cobalt(II) oxalate dihydrate was found to reveal two endothermic and one exothermic effects under the same conditions (Fig. 1). The exothermic effect is evident to be due to the reaction (4) which undergoes in helium containing remaining O_2 .



No exothermic effects were found by decomposition either of supported $\text{Ni}(\text{COO})_2 \cdot 2\text{H}_2\text{O}$ or $\text{Fe}(\text{COO})_2 \cdot 2\text{H}_2\text{O}$. It indicates that no reaction (4) occurs in these cases although at least $\text{Fe}(\text{COO})_2 \cdot$ decomposes by CO evolution in accordance with the re-

action (3) [5]. So, the reaction (4) seems to have presumably a catalytic character. This conclusion is suggested by well-known catalytic properties of cobalt and cobalt oxides in respect with the above reaction.

An assignment of the reaction (4) to a catalytic type is suggested unambiguously by the decomposition of unsupported $\text{Co}(\text{COO})_2$. In helium, there are observed exothermal and endothermal effects in the range of thermal decomposition of $\text{Co}(\text{COO})_2$ (Fig. 2). The temperature ranges of the exothermal and endothermal effects of catalytic CO oxidation and decomposition of unsupported $\text{Co}(\text{COO})_2$, respectively, are not coincided in the low-oxygen atmosphere as it is shown in Fig. 2. In the range of the decay of the $\text{Co}(\text{COO})_2$, a DTG-trace in helium shows two peaks at 250–300 and 340–380°C indicating changes in the rate of the mass loss by the decomposition of $\text{Co}(\text{COO})_2$. The low-temperature pick on the DTG-trace at 250–300°C is due to a change in the rate of temperature enhancement owing heat release by catalytic CO oxidation. This peak is attributed to the exothermal effect on the DSC-trace. At higher temperature, there is no more oxygen to be consumed by the catalytic oxidation of CO and the CO catalytic oxidation gets to be controlled by the diffusive retardation in the static system. According to the TG-trace, the mass loss on this stage corresponds to the ‘normal’ temperature-programmed decomposition of the $\text{Co}(\text{COO})_2$ residue. This peak on the DTG-trace is only due to the endothermal effect of the $\text{Co}(\text{COO})_2$ decomposition.

In air, the exothermal effects are registered both for supported and for unsupported $\text{Co}(\text{COO})_2$. A typical TG- and DSC-traces for the decomposition of supported $\text{Co}(\text{COO})_2$ are shown in Fig. 3. In air, the decrease in the temperature range of the decomposition of $\text{Co}(\text{COO})_2$ supported on PC is probably connected with hyper-programmed overheating of the sample by the heat of the reaction (4) which provokes dramatically increase in the rate of the $\text{Co}(\text{COO})_2$ decay.

Another feature of the supported $\text{Co}(\text{COO})_2$ decomposition in low-oxygen atmosphere is the CoO formation by pyrolysis instead of Co_3O_4 yielded by the $\text{Co}(\text{COO})_2$ decomposition in air. Observed ratio of the mass loss at the decomposition step to that of the dehydration of $\text{Co}(\text{COO})_2$ is 0.509 which is in accordance with a theoretic one (0.503). These data indicate that the pyrolysis of supported $\text{Co}(\text{COO})_2$ in the presence of helium containing traces of O_2 follows the reaction (3).

Magnetic moment measurements suggest this conclusion. The nanoparticles of Fe_2O_3 , CoO (Co_3O_4) and NiO populated the interspheric voids of the photonic crystals exhibited no ferromagnetic effects indicating that no metallic inclusions or other ferromagnetic phases were formed by the thermal decomposition of metal(II) oxalates in helium in the presence of O_2 traces. However, the reduction of the re-

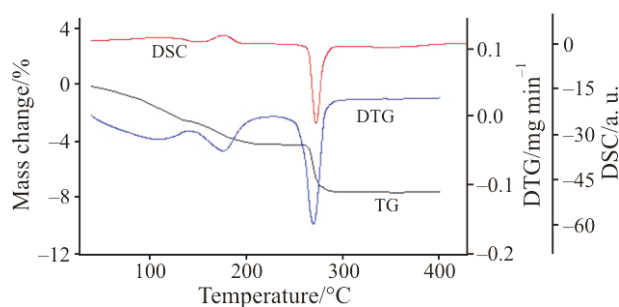


Fig. 3 TG, DTG and DSC plots for the pyrolysis of $\text{Co}(\text{COO})_2 \cdot 2\text{H}_2\text{O}$ supported on the photonic crystals based on SiO_2 (in air); heating rate is 5 K min^{-1}

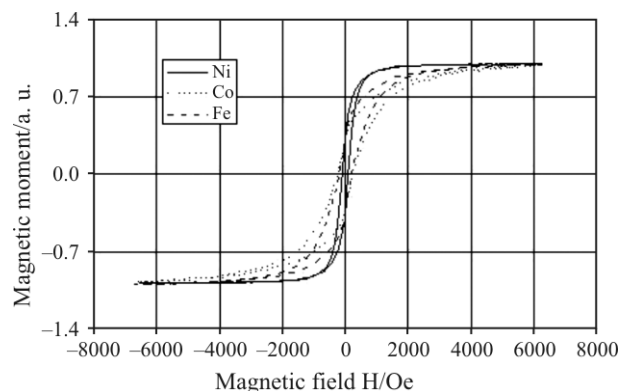


Fig. 4 Plots of magnetization vs. magnetic field (H) for the photonic crystals modified with the products of the thermal decomposition of $\text{M}(\text{COO})_2 \cdot 2\text{H}_2\text{O}$ [$\text{M}=\text{Fe}, \text{Co}, \text{Ni}$] within the interspheric voids at room temperature

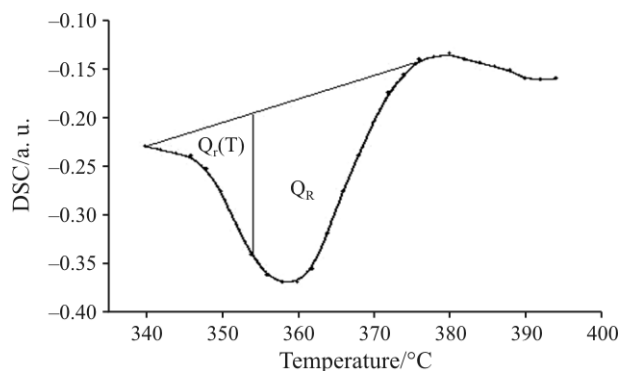


Fig. 5 DSC-curve for the decomposition of supported $\text{Co}(\text{COO})_2$ in the temperature range 340–380°C in helium atmosphere; heating rate is 5 K min^{-1}

sulting samples with H_2 at appropriate temperatures revealed unambiguous evidence for the formation of the ferromagnetic phases (Fig. 4).

It is noteworthy to analyze the kinetics of the supported $\text{Co}(\text{COO})_2$ decomposition in low-oxygen atmosphere using the DSC-data in the range of temperatures from 345 to 380°C (Fig. 5). In this interval there is no influence of the exothermal effect of the catalytic oxidation of CO by oxygen the endothermal effect of anhydrous cobalt(II) oxalate. The form of the kinetics is

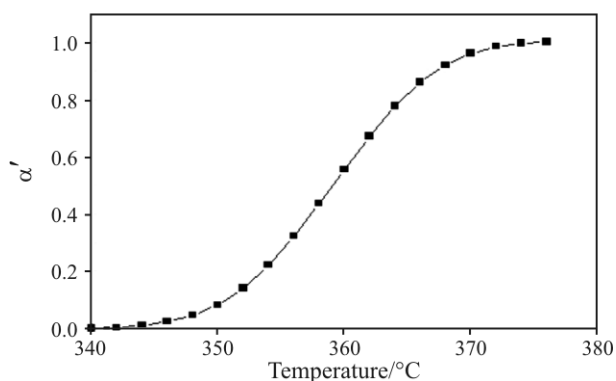


Fig. 6 The fractional decomposition α' of anhydrous cobalt(II) oxalate supported on PC based on SiO_2 as a function of temperature in He; heating rate is 5 K min^{-1}

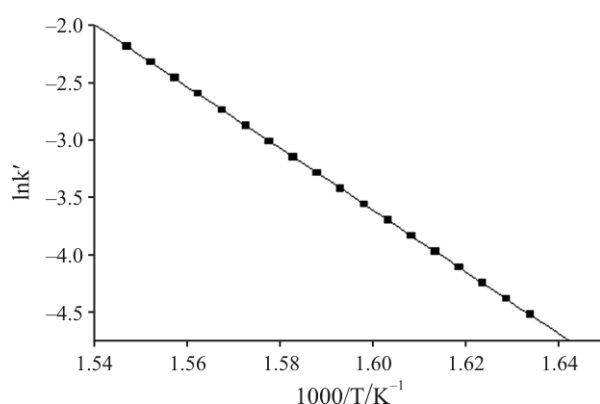


Fig. 7 Arrhenius plots for the thermal decomposition of $\text{Co}(\text{COO})_2$ supported on PC based on SiO_2 in the temperature range $340\text{--}380^\circ\text{C}$ in helium atmosphere; heating rate is 5 K min^{-1}

shown in Fig. 6 where the fractional decomposition α' of $\text{Co}(\text{COO})_2 \cdot 2\text{H}_2\text{O}$ supported on the photonic crystals is shown as a function of temperature. The initial decay process commences as soon as the sample reaches the temperature of the beginning of the reaction (3) and is followed, after an induction period, by the acceleratory reaction connected with the catalytic CO oxidation. Denoting the fractional decomposition at the end of the reaction (4) by α_0 , then the fraction of $\text{Co}(\text{COO})_2$ decomposed in the succeeding 'normally-programmed' process is $\alpha' = \alpha/\alpha_0$.

The remainder of the reaction from $\alpha=0.6$ to 0.95 is fitted by the Avrami–Erofeev equation with $n=2$, i.e.,

$$1 - \alpha' = \exp[-k\alpha'(t - t_0')^2] \quad (5)$$

where t_0' is the time of the decomposition of $\text{Co}(\text{COO})_2$ accompanied by catalytic CO oxidation on the product of the $\text{Co}(\text{COO})_2$ decay.

The fractional decomposition α' was calculated by the endothermal effect of the DSC-trace observed in the range $345\text{--}380^\circ\text{C}$ (Fig. 5) as

$$\alpha' = \frac{Q_r}{Q_R}$$

where Q_r is the partial heat of the $\text{Co}(\text{COO})_2$ decomposition registered by the temperature T and Q_R is the total heat effect of the reaction.

The Arrhenius plot is presented in Fig. 7. Equation (5) holds over the range $0.6 < \alpha < 0.95$. The Arrhenius equation for the decomposition of the $\text{Co}(\text{COO})_2$ is

$$\ln(k'/\text{min}^{-1}) = 39.3 - 26800/RT$$

The activation energy over this period of the $\text{Co}(\text{COO})_2$ decomposition is $222.8 \text{ kJ mol}^{-1}$. This value is in accordance with the data obtained for isothermal decomposition of $\text{Co}(\text{COO})_2$ in a vacuum [2].

Conclusions

The thermal decomposition of $\text{Fe}(\text{COO})_2 \cdot 2\text{H}_2\text{O}$, $\text{Co}(\text{COO})_2 \cdot 2\text{H}_2\text{O}$ and $\text{Ni}(\text{COO})_2 \cdot 2\text{H}_2\text{O}$ obtained by in situ synthesis within the voids of the PC as nanoparticles under static conditions in helium containing remaining oxygen yielded oxides of the corresponding metal supported on the solid. The decay of $\text{Co}(\text{COO})_2 \cdot 2\text{H}_2\text{O}$ only was observed to show exothermal effect due to catalytic oxidation of CO by the traces of O_2 in helium. In the presence of air the decomposition of $\text{Co}(\text{COO})_2 \cdot 2\text{H}_2\text{O}$ supported on PC occurred at lower temperature. There is no endothermal effect which is masked on the DSC-traces of the $\text{Co}(\text{COO})_2 \cdot 2\text{H}_2\text{O}$ decomposition by exothermal oxidation of CO.

References

- 1 Patent RF No 2 296 100.
- 2 D. Broadbent, D. Dollimore and J. Dollimore, *J. Chem. Soc. A*, (1966) 1491.
- 3 V. A. Sharov, V. A. Zhilyaev, E. A. Nikonenko and T. M. Zhdanovskikh, *Koord. Khim.*, 6 (1980) 431.
- 4 B. Małecka, E. Drozd-Cieśla and A. Małecka, *J. Therm. Anal. Cal.*, 68 (2002) 819.
- 5 V. P. Kornienko, *Ukr. J. Chem.*, 23 (1957) 159.
- 6 E. D. Macklen, *J. Inorg. Nucl. Chem.*, 30 (1968) 2689.
- 7 D. Broadbent, D. Dollimore and J. Dollimore, *J. Chem. Soc. A*, (1966) 278.

DOI: 10.1007/s10973-008-9024-0